Redundancy Resolution of Kinematically Redundant Parallel Manipulators Via Differential Dynamic Programing

João Cavalcanti Santos, Maíra Martins Da Silva

Redundancy Resolution of Kinematically Redundant Parallel Manipulators via Differential Dynamic Programming

João Cavacanti Santos
PhD Student
School of Eng. of São Carlos
Dept. of Mechanical Engineering
University of São Paulo
São Carlos - SP, Brazil
Email: joao.cavalcanti.santos@usp.br

Maíra Martins da Silva*
Professor
School of Eng. of São Carlos
Dept of Mechanical Engineering
University of São Paulo
São Carlos - SP, Brazil
Email: mairams@sc.usp.br

Kinematic redundancy may be an efficient way to improve the performance of parallel manipulators. Nevertheless, the inverse kinematic problem of this kind of manipulator presents infinite solutions. The selection of a single kinematic configuration among a set of many possible ones is denoted as redundancy resolution. Whilst several redundancy resolution strategies have been proposed for planning the motion of redundant serial manipulators, suitable proposals for parallel manipulators are seldom. Redundancy resolution can be treated as an optimization problem that can be solved locally or globally. Gradient projection methods have been successfully employed to solve it locally. For global strategies, these methods may be computationally demanding and mathematically complex. The main objective of this work is to exploit the use of Differential Dynamic Programming (DDP) for decreasing the computational demand and mathematical complexity of a global optimization based on the gradient projection method for redundancy resolution. The outcome of the proposed method is the optimal inputs for the active joints for a given trajectory of the end-effector considering the input limitations and different cost functions. Using the proposed method, the performance of a redundant 3PRRR manipulator is investigated numerically and experimentally. The results demonstrate the capability and versatility of the strategy.

*Corresponding author.

1 Introduction

Due to their kinematic architecture, parallel kinematic machines (PKMs) possibly present higher stiffness [1], higher dynamic performance [2, 3] and higher accuracy [4] compared to serial ones. Whilst these characteristics may be interesting for industrial applications, PKMs suffer from important drawbacks such as the presence of singularities [5,6], the limited workspace [6], the complex control strategies' requirements [7–10], among other issues.

A strategy for dealing with the presence of singularities and workspace limitations is the introduction of an extra active joint in an active kinematic chain [11, 12]. This strategy is denoted as kinematic redundancy. The kinematically redundant parallel manipulators present higher mobility than required for the desired task allowing the avoidance of singularities and obstacles [13], enlarging the usable workspace [6,14]. In addition, kinematically redundant parallel manipulator might present higher accuracy [15], better motion/force transmissibility [16], improved dynamic performance [2, 3], enhanced energy efficiency [17] and optimized manipulability [18] compared to the non-redundant ones.

Figure 1 depicts the kinematically redundant planar parallel manipulator 3PRRR built at São Carlos School of Engineering at University of São Paulo. This manipulator presents three kinematic chains composed of one active prismatic joint (P), one active revolute joint (R) and two passive revolute joints (RR). This versatile setup can be exploited to study the non-redundant manipulator 3RRR by locking the prismatic joints and to study the redundant manipulators

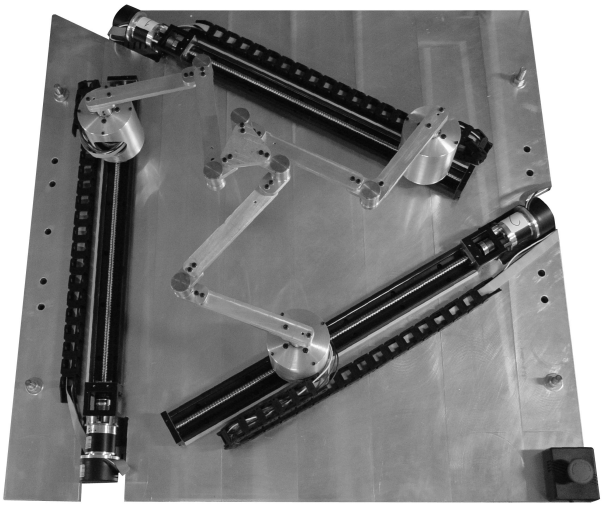

Fig. 1: 3PRRR: the kinematically redundant planar parallel manipulator built at São Carlos School of Engineering at University of São Paulo

PRRR+2RRR, 2PRRR+RRR and 3PRRR by actuating the prismatic joints.

Due to the kinematic redundancies, the inverse kinematic problem presents infinite solutions [19]. In other words, there are infinite possible active joint inputs for a single end-effector's pose. As posed in [11], the problem of selecting a single configuration among a set of many possible ones when dealing with inverse kinematics of redundant manipulators can be denoted as redundancy resolution. Redundancy resolution can be treated as an optimization problem that can be solved locally or globally [11]. The former approaches address the problem by considering kinematic relations between the inputs of the active joints and the outputs of the end-effector (the end-effector's pose). These relations can be formulated using gradient projection methods, Jacobian based strategies, among others [19]. They can be implemented online and are able to take into account varying constraints and/or moving obstacles. The latter approaches seek to find optimal inputs for the active joints for a given trajectory of the end-effector. These methods, also denoted as tracking problems [11], aim to optimize a cost function along the entire pre-defined trajectory.

Redundancy resolution has been extensively exploited for redundant serial manipulators [20–22]. For instance, a global approach has been successfully implemented to a seven-DOF serial manipulator in [11]. Using a multi-criteria optimization and the Fast Non-Dominated Sorting Genetic Algorithm (see NSGA-II at [23]), Marcos, Machado and Azevedo-Perdicolis [24] have numerically studied the redundancy resolution of the planar serial RRRR robot. A local approach has been exploited in [25] to resolve the human arm redundancy. Moreover, Kim *et al.* [25] have employed this approach for controlling an upper limb 7-DOF wearable exoskeleton robot. Recently, Minami, Matsuno and Yanou [26] have used global optimization algorithms to design and control a redundant serial robot using the concept of dynamic reconfiguration manipulability.

Regarding PKMs, the use of kinematic redundancy and redundancy resolution have also been treated in some works. Among them, Kotlarski *et al.* [27] and Thanh *et al.* [28] have proposed optimization strategies to deal with the redundant input for the PRRR+2RRR, a redundant manipulator with a single level of kinematic redundancy, using a global redundancy resolution approach. Extra levels of redundancies have been numerically treated in [12] and [3]. On the one hand, Cha, Lasky and Velinsky [12] have resolved the inputs of the redundant actuators of the 3PRRR using a local redundancy resolution approach. For that, these authors have posed an optimization problem that maximizes the absolute value of the determinant of the Jacobian matrix that corresponds to a forward kinematic singularity. On the other hand, Fontes and da Silva [3] have studied the impact of extra levels of redundancies in the dynamic performance of the 3PRRR via a global redundancy resolution approach and dynamic indexes depicted in the workspace. For that, an optimization problem was posed minimizing the maximum required torque to perform a pre-defined trajectory. In order to improve the force capabilities and to avoid singularities, Boudreau and Nokleby [29] have numerically exploited kinetostatic analysis to plan the motion of the redundant actuators of the 3PRPR via a local optimization problem. Despite numerical evidences that the use of extra levels of kinematic redundancies can satisfactorily improve the dynamic performance and enlarge the workspace [3], experimental studies are scarce.

Redundancy resolution for manipulators with several levels of kinematic redundancy is generally formulated as a cumbersome optimization problem. This is particularly true for PKMs due to the complexity of the kinematic relations. Due to this fact, most attempts to tackle this problem are based on global approaches that seek the optimal parameters for a polynomial description of the trajectory [3, 27]. Moreover, this approach lacks versatility due to this description.

In this manuscript, a simple, yet versatile, global redundancy resolution approach is proposed. Global approaches are know to be expensive computationally [19]. To tackled this issue, a gradient projection method is firstly employed for deriving an optimal global motion. The outcome of this strategy may demand unrealistic input values by imposing high acceleration values. To overcome this issue, Differential Dynamic Programming (DDP) [30] is used to minimize the difference between the practical global motion from the optimal global motion while acceleration values are kept limited. The proposed approach is versatile, being a good option for redundancy resolution of manipulators with several levels of kinematic redundancy.

This manuscript is organized as follows. Section 2 describes the proposed motion planning strategy. The proposed strategy is exploited for the motion planning of the redundant manipulator 3PRRR (see Fig. 1) in Section 3. Numerical and experimental results are discussed in Section 4. Finally, conclusions are drawn in Section 5.

2 Motion Planning Strategy

The proposed redundancy resolution strategy is based on the use of the outcome of the gradient projection method as an optimal global motion. Whilst gradient projection methods work well for local approaches, unrealistic input values can be derived if this method is exploited for global approaches. This issue is tackled by using the DDP to minimize the difference between this optimal global motion and a practical one by a proper selection of the weighting terms of the optimization.

A similar approach has been proposed in [31] for redundant serial manipulators using DDP. In this case, Guigue *et al.* [31] considers two cost functions, the joint speed norm and the aerodynamic interference. PKMs present different challenges from the ones faced in [31]. In this way, different cost functions are proposed and evaluated hereafter.

2.1 Redundancy Resolution

On the one hand, the direct kinematic problem seeks to find the task space trajectory $\mathbf{x}(t)$ for a given joint space trajectory, $\mathbf{x}(t) = f(\mathbf{q}(t))$. On the other hand, the inverse kinematic problem seeks the joint space trajectory $\mathbf{q}(t)$ that solves $\mathbf{x}(t) = f(\mathbf{q}(t))$. For a kinematically redundant manipulator, the inverse kinematic problem presents infinite solutions. Strategies for selecting a solution for this problem may consider different aspects such as: energy consumption, singularity avoidance, among others. These strategies may be posed as optimization problems. This is the case of gradient projection methods that have been revised in [19].

Considering a kinematically redundant manipulator with N degrees-of-freedom and M joints, a relation between the joints' velocities, $\dot{\mathbf{q}} \in \mathbb{R}^M$, and end-effector's velocities, $\dot{\mathbf{x}} \in \mathbb{R}^N$ can be derived. This relation can be formulated as:

$$\dot{\mathbf{q}} = \mathbf{J}^{\dagger}(\mathbf{q})\,\dot{\mathbf{x}}, \tag{1}$$

where $\mathbf{J}^{\dagger} \in \mathbb{R}^{M\times N}$ is the Moore-Penrose pseudoinverse of the Jacobian matrix. This approach minimizes the norm of the joint velocities, due to the properties of $\mathbf{J}^{\dagger}$. Nevertheless, this solution may yield joint space trajectories near singularity regions. The reason for this relies on the fact that the joint velocities are only minimized locally. This important drawback can be tackled by modifying the aforementioned relation [19]:

$$\dot{\mathbf{q}} = \mathbf{J}^{\dagger}(\mathbf{q})\,\dot{\mathbf{x}} + \left(\mathbf{I} - \mathbf{J}^{\dagger}\mathbf{J}\right)\dot{\mathbf{q}}_0, \tag{2}$$

where $\dot{\mathbf{q}}_0 \in \mathbb{R}^N$ is an arbitrary joint velocity vector. The element $\left(\mathbf{I} - \mathbf{J}^{\dagger}\mathbf{J}\right)$ projects any vector into the null space. Therefore, the second parcel of eq. 2 is a vector with components of a general $\dot{\mathbf{q}}_\mathbf{0}$ which does not produce motion into the task space. Choosing a cost function $H(\mathbf{q})$, this optimization problem can be solved using the gradient projection method yielding $\dot{\mathbf{q}}_0 = \nabla H(\mathbf{q})$. This procedure finds a joint space trajectory $\mathbf{q}(t)$ which produces the demanded task space trajectory $\mathbf{x}(t)$ optimizing joint velocities $\dot{\mathbf{q}}$ (eq. 1) and the cost function $H(\mathbf{q})$. In this way, using this strategy, joint velocities will be optimized under the perspective of $H(\mathbf{q})$, which may be any differentiable function.

Equations 1 and 2 solve the optimization problem locally. Nevertheless, many applications in robotics present a previously known task space trajectory, $\mathbf{x}(t)$. For a global optimization strategy, optimal control theory, dynamic programming and calculus of variations have been exploited [20–22]. In this case, the optimization problem would seek the minimization of a cost function $H(\mathbf{q})$ for the entire task. This approach is known to require more complex mathematical tools as the Pontryagin's Maximum Principle [21, 32] or Bellman's Optimality Principle [33].

2.2 Differential Dynamic Programming

The use of DDP for trajectory planning taking into account input limitations has been employed in [34], among others. Redundancy resolution brings other challenges to trajectory planning problems. The main objective of this work is to exploit the use of DDP for decreasing the computational demand and mathematical complexity of a global optimization based on the gradient projection method for redundancy resolution.

It is widely known that the main objective of the DDP is the optimization of the sum of cost functions of a multistage problem. In this work, DDP is exploited to minimize the tracking error and accelerations for a given trajectory performed by a kinematically redundant PKM. The use of DDP for trajectory planning requires the discretization of the function that described the trajectory to be planned. In this way, the trajectory can be described as a discrete function $\boldsymbol{\zeta}(k)$ over discrete time instants $t_k = t(k)$ where $k = 0 \ldots n-1$. In this work, this trajectory should follow a given reference $\boldsymbol{\zeta}_r(k)$. During this motion, the tracking error, $\boldsymbol{\zeta}_r(k) - \boldsymbol{\zeta}(k)$, and the acceleration values, $\mathbf{a}(k)$ should be minimized. The cost function of this multiobjective optimization problem at the time instant t_k may be stated as

$$l(\boldsymbol{\zeta}(k), \mathbf{a}(k)) = c_r \left\|\boldsymbol{\zeta}_r(k) - \boldsymbol{\zeta}(k)\right\|^2 + c_a\, \mathbf{a}(k)^T\, \mathbf{a}(k), \tag{3}$$

where c_r and c_a are weighting factors that attribute the relevance among the tracking error and the acceleration values, respectively. The acceleration values, $\mathbf{a}(k)$, are the second order finite approximation of $\boldsymbol{\zeta}(k)$.

This optimization procedure should guarantee that at the end of the movement, the manipulator presents null velocity and acceleration. In order to satisfy this requirement, a final cost function for the final instant t_n is stated penalizing these non-null values:

$$\begin{aligned} l_f(\boldsymbol{\zeta}(n), \mathbf{v}(n), \mathbf{a}(n)) = c_r \left\|\boldsymbol{\zeta}_r(n) - \boldsymbol{\zeta}(n)\right\|^2 + \ldots \\ \ldots + c_{fv}\, \mathbf{v}(n)^T\, \mathbf{v}(n) + c_{fa}\, \mathbf{a}(n)^T\, \mathbf{a}(n), \end{aligned} \tag{4}$$

where $\mathbf{v}(k)$ is the finite difference approximation of the first order derivative of $\boldsymbol{\zeta}(k)$. The constants c_{fv} and c_{fa} should

have high values in order to guarantee negligible values of $\mathbf{v}(n)$ and $\mathbf{a}(n)$.

One can see that the input variables, $\boldsymbol{\zeta}(k)$, $\mathbf{v}(k)$ and $\mathbf{a}(k)$, are related by finite difference approximations. As a result, the argument of the optimization can be described by the Jerk vector $\mathbf{j}(k)$, that can be described by the third order finite approximation of $\boldsymbol{\zeta}(k)$. The remaining functions are integrated numerically based on their initial values $\boldsymbol{\zeta}(0)$, $\mathbf{v}(0)$ and $\mathbf{a}(0)$. Using this approach, the acceleration values are considered to be state variables. Moreover, the DDP's notation requires the definition of state variables and inputs. In this way, the state variables can be described by the vector $\mathbf{x}_k = [\boldsymbol{\zeta}(k)^T \ \mathbf{v}(k)^T \ \mathbf{a}(k)^T]^T$, and the inputs by the vector $\mathbf{u}_k = \mathbf{j}(k)$.

Using Euler integration, the state $\mathbf{x_{k+1}}$ can be described by a linear combination of the state vector $\mathbf{x_k}$ and the input vector $\mathbf{u}_k$:

$$\mathbf{x}_{k+1} = \mathbf{f}(\mathbf{x}_k, \mathbf{u}_k) = \mathbf{A}_k\mathbf{x}_k + \mathbf{B}_k\mathbf{u}_k, \tag{5}$$

where $\mathbf{f}$ is a vector function, $\mathbf{A}_k$ is the state matrix and $\mathbf{B}_k$ is the input matrix. Collecting the input vectors at every time instant in the matrix $\mathbf{U} = \{\mathbf{u}_0, ..., \mathbf{u}_{n-1}\}$, the total cost function $J(\mathbf{U}, \mathbf{x}_0)$ can be defined over the entire trajectory by the summation of the cost function defined by each time instant:

$$J(\mathbf{U}, \mathbf{x}_0) = l_f(\mathbf{x}_n) + \sum_{k=0}^{n-1} l(\mathbf{x}_k). \tag{6}$$

In other words, if the initial state vector $\mathbf{x}_0$ and the input vectors $\mathbf{U} = \{\mathbf{u}_0, ..., \mathbf{u}_{n-1}\}$ are available, not only the state vector $\mathbf{x}$ can be calculated through numerical integration but also the total cost J can be obtained. This process is called *Forward Pass* [30].

An optimization problem considering the variables $\mathbf{U}$ and $\mathbf{x}_0$ may be prohibitive due to its dimension. The Principle of Optimality [30] indicates that this problem can be divided into sub-problems at each time instant. Considering $\mathbf{U}_p = \{\mathbf{u}_p, ..., \mathbf{u}_{n-1}\}$ as sub-set of $\mathbf{U}$ containing its last $n-p$ vectors, a partial cost $J_p(\mathbf{U}_p, \mathbf{x}_p)$ can be calculated as

$$J_p(\mathbf{U}_p, \mathbf{x}_p) = l_f(\mathbf{x}_n) + \sum_{k=p}^{n-1} l(\mathbf{x}_k). \tag{7}$$

The function V_p can be defined as the minimum J_p possible for a given $\mathbf{x}_p$. This function, that is also known as cost-to-go function, can be described by the following optimization problem:

$$V_p(\mathbf{x}_p) = \min_{\mathbf{U_p}} \left\{ l_f(\mathbf{x}_n) + \sum_{k=p}^{n-1} l(\mathbf{x}_k) \right\}. \tag{8}$$

Thanks to the Principle of Optimality [30], if the following value of the V_{p+1} is already calculated, the value of V_p can be easily found:

$$V_p(\mathbf{x}_p) = \min_{\mathbf{U_p}} \Big\{ l(\mathbf{x}_p) + V_{p+1}\big(\mathbf{f}(\mathbf{x}_p, \mathbf{u}_p)\big) \Big\}. \tag{9}$$

Using this strategy, the procedure starts by the calculation of $V_n(\mathbf{x}_n) = l_f(\mathbf{x}_n)$. Then, at every stage p, the procedure seeks $\mathbf{u}_p$ that minimize V_p. This process is called *Backward Pass*. Since l, l_f and $\mathbf{f}$ are quadratic functions of state and input vectors, these optimization sub-problems can be solved using Sequential Quadratic Programming (SQP) [35], for instance. At every stage p, the outcome of this procedure is the minimization of the cost function by finding the optimal jerk vector (the input vector $\mathbf{u}_p$) and the derivation of the state vector by considering the optimal jerk vector and the former velocities and positions (see Eq. 5).

2.3 Global Optimization

The gradient projection method is an efficient local strategy for redundancy resolution [19]. This advantage can also be exploited for proposing a global and versatile strategy. Considering a kinematically redundant planar manipulator with N_r redundant actuators, the vector $\mathbf{q}_r \in \mathbb{R}^{N_r}$ can be defined containing the redundant joint inputs (angular or translational displacements). The time derivative of the input values of the redundant actuators, $\dot{\mathbf{q}}_r$, are selected to be the arbitrary joint velocity vector, $\dot{\mathbf{q}}_0$ in Eq. 2. In this way, these values can be derived through the gradient projection method:

$$\dot{\mathbf{q}}_r = \dot{\mathbf{q}}_0 = \nabla H(\mathbf{q}_r) \tag{10}$$

where H is a cost function that considers relevant aspects of the studied manipulator.

For a given cost function H, the input values of the redundant actuators, $\dot{\mathbf{q}}_r$, are calculated using the Gradient Projection Method. This approach would require the best pose of the redundant manipulator for every instant. This requirement could demand unfeasible accelerations and input torques. To overcome this issue, the DDP is exploited in order to attain reasonable joint inputs by a proper selection of the weighting factors of Eqs. 3 and 4. In order to do so, the input values of the redundant actuators $\dot{\mathbf{q}}_r$ are used as reference for the redundant actuators and a numerical investigation is carried out for assessing the maximum acceleration values. The DDP demands the discretization of these values. This discretization yields the reference $\boldsymbol{\zeta}_r$ in the DDP's scheme (see Eqs. 3 and 4).

The outcome of the DDP is the actual input values of the redundant actuators, $\boldsymbol{\zeta}$. The proposed scheme is considered versatile since the designer can exploit the weighting factors of Eqs. 3 and 4 to limit the manipulator's accelerations. This limitation would impact the tracking performance of the manipulator.

Once determined, the input values of the redundant actuators $\boldsymbol{\zeta}$ can be used for the derivation of the input values of all actuators $\boldsymbol{\Theta}$, non-redundant and redundant ones. This can

be done since the kinematic model presents a unique solution for a given configuration of the redundant actuators $\boldsymbol{\zeta}$ and a given end-effector's pose $\mathbf{X}$.

3 The Case Study: 3PRRR

The proposed methodology is applied for the derivation of the inputs for the redundant actuators of a kinematically redundant planar parallel manipulator, the 3PRRR. In order to do so, the kinematic model and the cost function should be fully derived. These steps are described in this section. Firstly, the experimental setup is described in Section 3.1. Secondly, the kinematic model is derived in Section 3.2. Finally, the definition of the cost function is addressed. Regarding PKMs, different aspects should be considered to build such cost function, such as manipulability, rigidity, dynamic isotropy, among others [36]. In this work, the cost function H (see Eq. 10) is defined as a weighted sum of distinct cost functions in order to consider some important design tradeoffs of PKMs.

3.1 Setup Description

The proposed redundancy resolution approach is applied on a 3PRRR, a planar parallel robot with 3 kinematic chains actuated by six servomotors depicted in Fig. 1. Each kinematic chain includes an active prismatic joint and an active revolute joint. The actuation of the prismatic joints allow the manipulator's reconfiguration. The actuation of the prismatic and revolute joints is performed by brushless Maxon EC60 flat motors. The nominal torque of these motors is 0.257N.m @ 3580rpm. These motors are coupled with Maxon planetary gearhead GP52C with a reduction rate of 3.5:1. The resulting available nominal torque of the set is 0.82N.m @ 1200rpm. The linear motion is performed by three table systems with ball screw HIWIN KK60-10-C-E-600-A-1-F0-S3. Their stroke range is 600mm and their pitch is 10mm. Each motor is controlled by an individual controller board Maxon EPOS2 50/5. The nominal current and maximum voltage of these boards are 5A and 50 VDC, respectively. The communication between the boards is via CAN protocol and the communication with the computer is via USB port.

Several control strategies, denoted as *Modes*, are available in these boards. The experimental campaign described hereafter exploited the *Interpolated Position Mode*. In this mode, the user provides the desired positions and velocities at diverse time instants. This data is interpolated through splines by the board and is used as a reference signal to the control strategies. Moreover, in this mode, linear position feedforward and position feedback control strategies are used to guarantee performance and robustness. The control parameters, the feedforward and feedback gains, have been adjusted manually.

Figure 2 shows a schematic representation of the planar manipulator, depicting the kinematic parameters. On the one hand, as aforementioned the manipulator presents six actuators, the active revolute joints θ_i and the active prismatic joints ζ_i where i represents each kinematic chain ($i = 1 \ldots 3$). On the other hand, the end-effector presents three DOFs described by the coordinates x, y and α. The revolute joints B_i and C_i are passive ones. The lengths of links A_iB_i and B_iC_i are, respectively, l_2 and l_3. The angles γ_i represent the orientation of each prismatic joint. The orientation of the link B_iC_i is β_i. The length h is the distance between the centroid of the end-effector and the point C_i. A coordinate system $O-(x,y)$ is defined at the center of the manipulator. The distance between the origin of this coordinate system and the center of any prismatic actuator is a. Regarding the prototype dimensions, the numerical values of h, a, l_2 and l_3 are presented in Table 1. These values have also been used in the numerical evaluation.

Table 1: Dimensions of the prototype

h	a	l_2	l_3
59.7 mm	259.8 mm	191.0 mm	232.0 mm

3.2 Kinematic Model

In this subsection, the inverse kinematic models of the manipulators under study are fully derived. Moreover, the Jacobian matrix of this manipulator is also described. The outcome of the modelling procedure is exploited by the redundancy resolution approach proposed in this work. The kinematic parameters are depicted in Fig. 2 and have been previously described. The modeling approach can be exploited for the derivation of the kinematic models for the non-redundant 3RRR manipulator and the redundant 2RRR+PRRR ($N_r = 1$), RRR+2PRRR ($N_r = 2$) and 3PRRR ($N_r = 3$) manipulators.

3.2.1 Inverse Kinematics

The Inverse Kinematic Model (IKM) of a robotic manipulator attempts to calculate the active joints' positions $\boldsymbol{\Theta}$ for a given end-effector's position $\mathbf{X} = [x, y, \alpha]^T$. The IKM of the non-redundant manipulator relates the three active joints' positions $\boldsymbol{\Theta} = [\theta_1, \theta_2, \theta_3]$ with the end-effector's position. In this case, the solution of this problem is unique. The IKMs of the redundant manipulators attempt to correlate $N_r + 3$ active joints' positions $\boldsymbol{\Theta} = [\theta_1, \theta_2, \theta_3, \zeta_1, \ldots, \zeta_{N_r}]^T$ with the end-effector's position, where N_r is the number of redundant actuators. Due to the presence of kinematic redundancies, the IKM presents infinite solutions of $\boldsymbol{\Theta}$ for a given $\mathbf{X}$.

In this manuscript, a redundancy resolution scheme (see Section 2) is proposed for the definition of the inputs of redundant actuators, the inputs of active prismatic joints $\boldsymbol{\zeta} = [\zeta_1, \ldots, \zeta_{N_r}]^T$. In this way, for given $\mathbf{X}$ and $\boldsymbol{\zeta}$, the inverse kinematic problem described hereafter aims to determine the input values θ_1, θ_2 and θ_3.

To do so, the geometrical relation regarding the length of the link B_iC_i of the kinematic chain i can be imposed (details

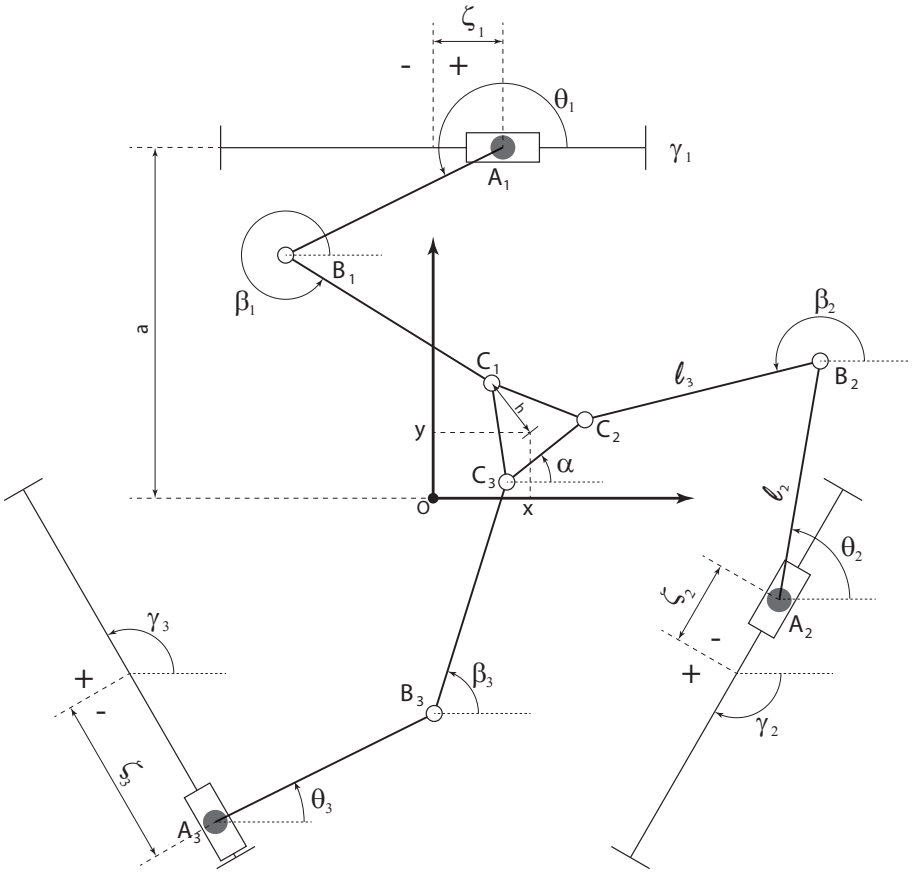

Fig. 2: Schematic representation of a 3PRRR

can be found in [2,3]):

$$||\mathbf{r_{C_i}} - \mathbf{r_{B_i}}||^2 = \left\| \begin{bmatrix} \rho_{xi} - l_2 \cos\theta_i \\ \rho_{yi} - l_2 \sin\theta_i \end{bmatrix} \right\|^2 = l_3^2, \tag{11}$$

where $\mathbf{r_{B_i}}$ and $\mathbf{r_{C_i}}$ are the position vectors of the points B_i and C_i, respectively. Moreover, ρ_{xi} and ρ_{yi} can be defined as

$$\begin{aligned} \begin{bmatrix} \rho_{xi} \\ \rho_{yi} \end{bmatrix} = \begin{bmatrix} x \\ y \end{bmatrix} + h \begin{bmatrix} \cos(\alpha + \gamma_i \pm \pi/2) \\ \sin(\alpha + \gamma_i \pm \pi/2) \end{bmatrix} - \dots \\ \dots + \zeta_i \begin{bmatrix} \cos\gamma_i \\ \sin\gamma_i \end{bmatrix} - a \begin{bmatrix} \cos(\gamma_i \pm \pi/2) \\ \sin(\gamma_i \pm \pi/2) \end{bmatrix}. \end{aligned} \tag{12}$$

The signal of the term $\pm\pi/2$ is defined in function of the direction of the increment of ζ_i. For the specific case of Fig. 2, this sign is positive and the angle is $\gamma_i + \pi/2$.

Expanding the norm in Eq. 11, one can define the terms e_{1i}, e_{2i} and e_{3i} as

$$\begin{aligned} \underbrace{(-2.l_2.\rho_{yi})}_{e_{1i}} \sin\theta_i + \underbrace{(-2.l_2.\rho_{xi})}_{e_{2i}} \cos\theta_i + \dots \\ \dots + \underbrace{\rho_{xi}^2 + \rho_{yi}^2 + l_2^2 - l_3^2}_{e_{3i}} = 0. \end{aligned} \tag{13}$$

The transcendental Eq. 13 may be solved using the *Weierstrass substitution*:

$$\theta_i = 2\tan^{-1}\left(\frac{-e_{i1} \pm \sqrt{e_{i1}^2 + e_{i2}^2 - e_{i3}^2}}{e_{i3} - e_{i2}} \right). \tag{14}$$

Once θ_i is known, β_i can also be determined by the following expression:

$$\beta_i = \tan^{-1}\left(\frac{\rho_{yi} - l_2 \sin\theta_i}{\rho_{xi} - l_2 \cos\theta_i} \right). \tag{15}$$

3.2.2 Jacobian Matrix

Relevant information can be obtained by evaluating the Jacobian matrix of a manipulator at a given pose. This matrix can be determined by taking the time-derivative of the geometrical constraint described by Eqs. 11 and 13. For each kinematic chain i, this derivation leads to the following relation (details can be found in [2,3]):

$$\begin{aligned} \dot{x}\underbrace{[l_3\cos\beta_i]}_{a_{i,1}} + \dot{y}\underbrace{[l_3\sin\beta_i]}_{a_{i,2}} + \dot{\alpha}\underbrace{[l_3 h\sin(\beta_i - \gamma_i - \alpha \pm \pi/2)]}_{a_{i,3}} = \\ = \dot{\theta}_i\underbrace{[l_2 l_3\sin(\beta_i - \theta_i)]}_{b_{i,i}} + \dot{\zeta}_i\underbrace{[l_3\cos(\beta_i - \gamma_i)]}_{b_{i,m+3}}, \end{aligned} \tag{16}$$

where $m = 1 \ldots N_r$, according to the number of redundant actuators. The Jacobian matrix, $\mathbf{J}$, can be found by the matricial relation:

$$\dot{\mathbf{X}} = \mathbf{A}^{-1}\mathbf{B}\dot{\mathbf{\Theta}} = \mathbf{J}\dot{\mathbf{\Theta}}. \tag{17}$$

where $\mathbf{A} = (a_{i,j}) \in \mathbb{R}^{3\times3}$ and $\mathbf{X} = [x, y, \alpha]^T \in \mathbb{R}^{3\times1}$.

For the non-redundant 3RRR manipulator, $\mathbf{\Theta} = [\theta_1, \theta_2, \theta_3] \in \mathbb{R}^{3\times1}$, $\mathbf{B} = diag(b_{i,i}) \in \mathbb{R}^{3\times3}$ and $\mathbf{J} = \mathbf{A}^{-1}\mathbf{B} \in \mathbb{R}^{3\times3}$. For the redundant manipulators, $\mathbf{\Theta} = [\theta_1, \theta_2, \theta_3, \zeta_1, \ldots, \zeta_{N_r}]^T \in \mathbb{R}^{3+Nr\times1}$, $\mathbf{B} \in \mathbb{R}^{3\times3+Nr}$ is defined by

$$\mathbf{B} = \begin{bmatrix} b_{1,1} & 0 & 0 & b_{1,4} & \ldots & 0 \\ 0 & b_{2,2} & 0 & \vdots & \ddots & 0 \\ 0 & 0 & b_{3,3} & 0 & 0 & b_{3,m+3} \end{bmatrix}, \tag{18}$$

where $m = 1 \ldots N_r$ and $\mathbf{J} = \mathbf{A}^{-1}\mathbf{B} \in \mathbb{R}^{3\times3+N_r}$.

Several kind of singularities can occur if the matrices $\mathbf{A}$ or $\mathbf{B}$ are not full rank. Near singularity regions, the Jacobian matrix $\mathbf{J}$ becomes ill-conditioned. In this work, a major concern is when the matrix $\mathbf{A}$ is singular. In this case, displacements of $\mathbf{X}$ can happen even when the actuators are locked, yielding a loss of the manipulator's rigidity.

3.3 Definition of the cost function $H(\boldsymbol{\zeta})$

The cost function $H(\boldsymbol{\zeta})$, Eq. 10, for a given pose $\mathbf{X}$ of the end-effector should measure how convenient the positions of redundant actuators $\boldsymbol{\zeta}$ are. This measure may include manipulability, rigidity, dynamic isotropy, among others [36]. In this way, the definition of $H(\boldsymbol{\zeta})$ is dependent not only on the design requirements but also on the manipulator under study. This function can be defined as a weighted sum of several cost functions considering different aspects.

This work proposes the use of three cost functions for redundancy resolution of the redundant 3PRRR manipulator. Firstly, singularity regions are avoided by the evaluation of the singular values of the Jacobian matrix, $\mathbf{J}$ (see 17). This is considered by the cost function $H_1(\boldsymbol{\zeta})$. Secondly, the limits of the manipulator's workspace should be included. This can be done by imposing geometrical constraints. These constraints should impose upper and lower limits on the distance of the points A_i and C_i and on the redundant actuators' position ζ_i for each kinematic chain i. This constrained optimization problem can be written as an unconstrained optimization problem by using penalty methods [35]. The unconstrained problem is posed by the addition of penalty terms in the objective function. These penalty terms present high values when the constraint is violated. In this way, two cost functions are introduced to include the limitations of the manipulator's workspace. The constraint on the distance of the points A_i and C_i is described by the cost function $H_2(\boldsymbol{\zeta})$ and the constraint on the value of ζ_i is described by the cost function $H_3(\boldsymbol{\zeta})$. These functions are discussed hereafter.

3.3.1 Singular Value Decomposition of J

As discussed in Section 3.2.2, singularities have to be avoided. Figure 3 illustrates the 3RRR manipulator in two distinct configurations: (A) a non-singular configuration and (B) a singular configuration. Since the links B_iC_i are attached by passive revolute joints, they are only capable of transmitting forces through their lines of action, depicted by dashed lines in Fig. 3. Torque can be supported by the manipulator only if the intersections of the lines of action do not lie at the same point. If they lie at the same point as depicted in Fig. 3(B), no torque can be supported and the mechanism looses rigidity. Other singular configuration happens when the distal links are parallel and cannot sustain a force that is perpendicular to the links. For sake of brevity, this kind of singularity is not illustrated in this manuscript.

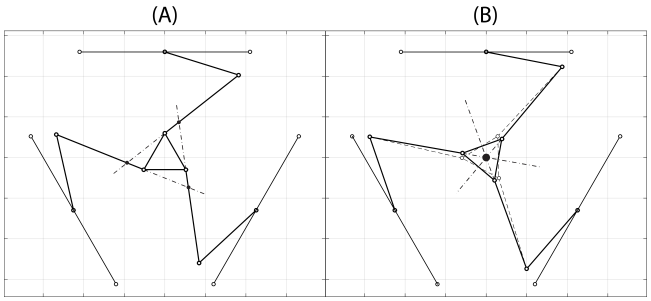

Fig. 3: 3RRR: (A) non-singular configuration and (B) singular configuration, which mitigates mechanism rigidity

Regions near to singular positions present ill-conditioned Jacobian matrices. In this way, a good strategy to avoid such regions is to evaluate the condition number of the Jacobian matrix and plan the motion in such a way that this number is as small as possible.

The Jacobian matrix of the redundant 3PRRR manipulator presents three singular values, $\sigma_1(\mathbf{J}) \gg \sigma_2(\mathbf{J}) \gg \sigma_3(\mathbf{J})$. For this case study, $\sigma_2(\mathbf{J})$ and $\sigma_3(\mathbf{J})$ are close to each other as illustrated in Fig. 4. In order to consider this particularity, the proposed cost function to evaluate the singular values of the Jacobian matrix includes the three singular values in the following manner:

$$H_1(\boldsymbol{\zeta}) = -\frac{\sigma_1\big(\mathbf{J}(\boldsymbol{\zeta})\big)}{\sigma_2\big(\mathbf{J}(\boldsymbol{\zeta})\big)\,\sigma_3\big(\mathbf{J}(\boldsymbol{\zeta})\big)}. \tag{19}$$

The proposed strategy consists of attempting to maximize H_1 values since the gradient of the cost function is exploited for redundancy resolution (see Eq. 10). As a consequence, σ_1, σ_2 and σ_3 are required to attain values as close to each other as possible. This approach avoids ill-conditioned Jacobian matrices.

3.3.2 Distance between A_i and C_i

The limits of the manipulator's workspace should also be considered for a successful redundancy resolution

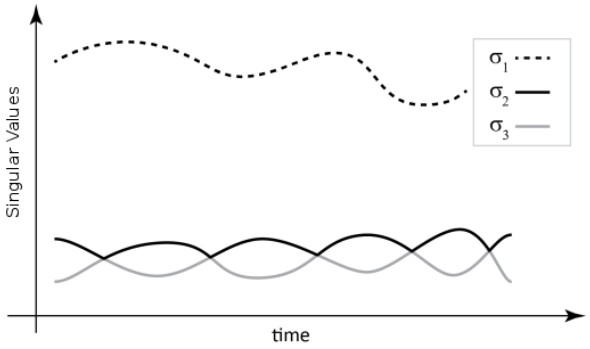

Fig. 4: Illustration of persistent interchange between σ_2 and σ_3

scheme. Kinematic constraints can be imposed by analysing the position vector $\mathbf{r}_{A_iC_i}$. The norm of this vector should be higher than $|l_2 - l_3|$ (the angle between the links is null) and smaller than $l_2 + l_3$ (the angle between the links is 180^o). In this way, a geometrical inequality constraint can be imposed:

$$|l_2 - l_3| \leqslant \|\mathbf{r}_{A_iC_i}\| \leqslant l_2 + l_3. \tag{20}$$

The use of such an inequality constraint is not straightforward regarding the proposed approach based on gradient projection. To overcome this issue, a cost function is defined via the introduction of penalty terms [35]. In order to do so, the strategy is to minimize the difference between a reference norm and the actual norm. The reference norm is considered to be $l_t = \sqrt{l_2^2 + l_3^2}$. Using this strategy, kinematic configurations where the angles θ_i and β_i are perpendicular are sought since they satisfy the constraint described by Eq. 20. In this way, the following cost function is proposed:

$$H_2(\boldsymbol{\zeta}) = -\sum_{i=1}^{3} \left(l_t - \|\mathbf{r}_{AC_i}\|\right)^2. \tag{21}$$

This cost function is maximized when $\|\mathbf{r}_{AC_i}\|$ is equal to l_t.

3.3.3 Limiting the amplitude of $\boldsymbol{\zeta}$

Finally, the limitation on the redundant actuators' position ζ_i for each kinematic chain i should be taken into account. This can be stated as $-\zeta_{max} \leqslant \zeta_i \leqslant \zeta_{max}$ (for this specific prototype $\zeta_{max} = 249.2$ mm). The following cost function is proposed to include these constraints in the redundancy resolution scheme:

$$H_3(\boldsymbol{\zeta}) = \sum_{i=1}^{3} \left(\frac{1}{\zeta_i - \zeta_{max}} - \frac{1}{\zeta_i + \zeta_{max}} \right). \tag{22}$$

One can realize that $(\zeta_i \to -\zeta_{max}^+) \Rightarrow (H_3 \to -\infty)$ and $(\zeta_i \to \zeta_{max}^-) \Rightarrow (H_3 \to -\infty)$. As a result, as ζ_i approaches to its limits, H_3 tends to $-\infty$, forcing ∇H to the other direction. This proposal keeps the constraints $-\zeta_{max} \leqslant \zeta_i \leqslant \zeta_{max}$ satisfied.

3.3.4 Final cost function

In this work, the proposed final cost function $H(\boldsymbol{\zeta})$ is the weighted sum of previously discussed cost functions. Thus,

$$H(\boldsymbol{\zeta}) = \sum_{k=1}^{3} c_k H_k(\boldsymbol{\zeta}), \tag{23}$$

where each H_k has been already defined and c_k is the weighting term of each cost function H_k, where $k = 1, \ldots, 3$.

The study of the physical meaning of these weighting terms enables one to tune their values appropriately via simulations. For instance, the constant c_3 defines how the constraint on the position of the redundant actuators is imposed. The upper and lower limits are satisfied for any value of $c_3 > 0$. Nevertheless, a numerical study clarifying how H_3 varies according to the c_3 can be valuable. Figure 5 shows this relation. On the one hand, low values of c_3 will require abrupt movements of the actuators. On the other hand, high values of c_3 promote smoother movements.

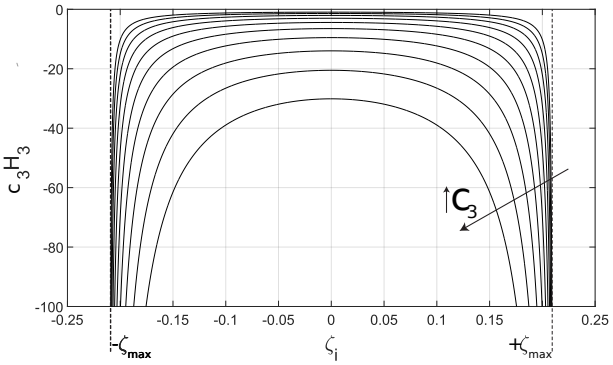

Fig. 5: The influence of c_3 over H_3

4 Results

The proposed redundancy resolution strategy has been exploited for the motion planning of a 3PRRR manipulator. The selected trajectory is a pick-and-place task illustrated in Fig. 6. Firstly, the manipulator leaves the 1^{st} pose (x_1, y_1, α_1) and reaches the 2^{nd} pose (x_2, y_2, α_2) in $1s$. Secondly, the manipulator leaves the 2^{nd} pose (x_2, y_2, α_2) and reaches the 3^{rd} one (x_3, y_3, α_3) in $1s$. The motion total duration should be $2s$. At these reference poses, the velocities and accelerations should be null. The pose vector is described by polynomials of 5^{th} degree for each interval of the motion. The coefficients of the polynomials can be found by solving definite integrals.

4.1 Singularities of the non-redundant 3RRR manipulator

During this pick-and-place task, the non-redundant manipulator 3RRR ($\boldsymbol{\zeta} = 0$) reaches singular configurations twice. Since this manipulator is not capable of avoiding singularities, it looses rigidity and it becomes sensitive to disturbances. A dynamic model of the 3RRR has been used for

evaluating the reference tracking capabilities of this manipulator during this pick-and-place task under a torque disturbance. The complete description of this dynamic model can be found in [2, 3]. Simulations have been carried out for a constant disturbance torque of -0.05 N.m applied to the end-effector during the pick-and-place task. Figure 7 illustrates the final reference pose (demanded) and the actual final pose calculated via numerical simulations. One can conclude that the non-redundant manipulator 3RRR was unable to reach the final pose under the considered disturbance.

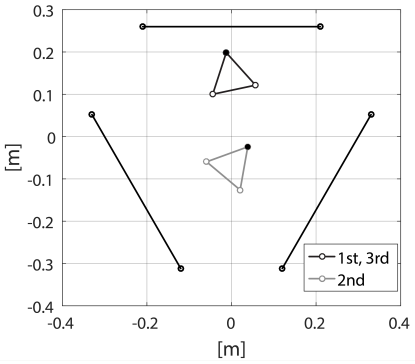

Fig. 6: Pick-and-place task: reference poses

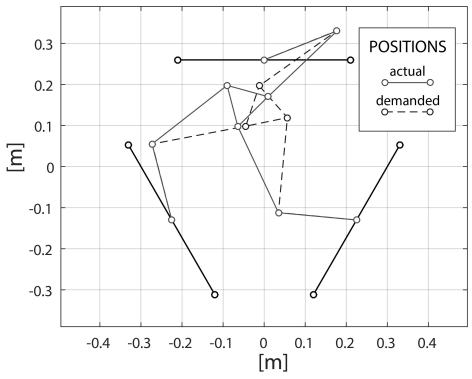

Fig. 7: Numerical results: comparison between the reference and actual poses of the non-redundant manipulator's end-effector under torque disturbance (-0.05 N.m)

Experimental tests have also been performed using the prototype described in Section 3.1. In order to evaluate the non-redundant 3RRR manipulator, the active translational joints (linear actuators) have been locked at the center of the linear guide. In this way, only the rotational actuators could be activated. The same pick-and-place task, depicted in Fig. 6, was performed under no load disturbance. Figure 8 shows two pictures of the prototype comparing the reference final pose and the actual final pose after performing the pick-and-place task. One can conclude that, once again, the non-redundant manipulator 3RRR was unable to reach the final pose experimentally due to the presence of singularities in the task's region.

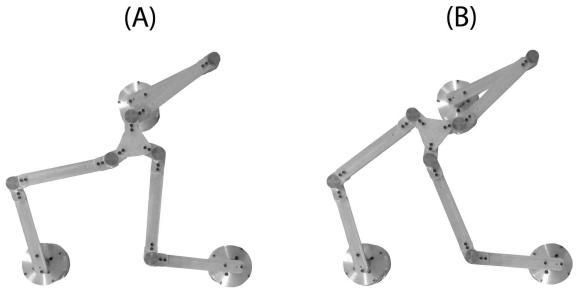

Fig. 8: Experimental results: comparison between (A) the reference final pose and (B) the actual final pose of the non-redundant manipulator under no load disturbance

4.2 Reconfiguration capabilities of the redundant 3PRRR

In this manuscript, extra levels of kinematic redundancies and a redundancy resolution scheme based on DDP are investigated in order to enhance the performance of a 3 degrees-of-freedom planar PKM. In this way, the kinematically redundant manipulator 3PRRR is exploited numerically and experimentally.

As previously described, a reference motion is obtained integrating eq. 10, with $H(\mathbf{q}_r)$ defined in eq. 23. The output of this step is $\mathbf{q}_r$, which presents proper positions for each instant separately, but may demand unrealistic accelerations. These input values for the redundant actuators are discretized yielding the reference $\boldsymbol{\zeta}_r$. This reference can be used in Eqs. 3 and 4. The outcome of the DDP's scheme is the motion of the manipulator according to the weighting terms of eqs. 3 and 4. These terms can be selected in such a way that the acceleration values are realistic according to the prototype and the tracking errors are acceptable. The numerical and experimental results described in this manuscript have been obtained using the weighting terms presented in Table 2. The tuning of the cost function weights was performed via extensive numerical simulations according to the design requirements of the manipulator under study.

Table 2: Weighting terms

c_1	c_2	c_3	c_r	c_a	c_{fv}	c_{fa}
0.75	75	0.025	2000	0.1	300	10^{16}

The time step of the DDP's scheme has been selected to be 2 ms, resulting in 10^3 sub-problems during the 2 s task.

Each sub-problem has been solved using SQP [35]. The termination tolerance on the function value, the global cost function J (eq. 6), has been defined as 10^{-10}. These parameters have been able to assure high precision for the global optimization problem.

The numerical evaluation of the reference tracking capabilities of redundant manipulator 3PRRR has been performed using a dynamic model. This model is fully described in [3]. Using this model, the pick-and-place task, depicted in Fig. 6, is numerically executed considering a constant disturbance torque of -1.30 N.m applied to the end-effector. Figure 9 shows the numerical comparison between the reference and actual pose of the redundant manipulator's end-effector. One can conclude that since the redundant manipulator has been capable of avoiding the singularities' regions, the manipulator's rigidity has been kept and the load disturbance has little impact on the manipulator's performance. It can be concluded that the redundant manipulator is less sensitive to load disturbances if an appropriate redundancy resolution scheme is selected.

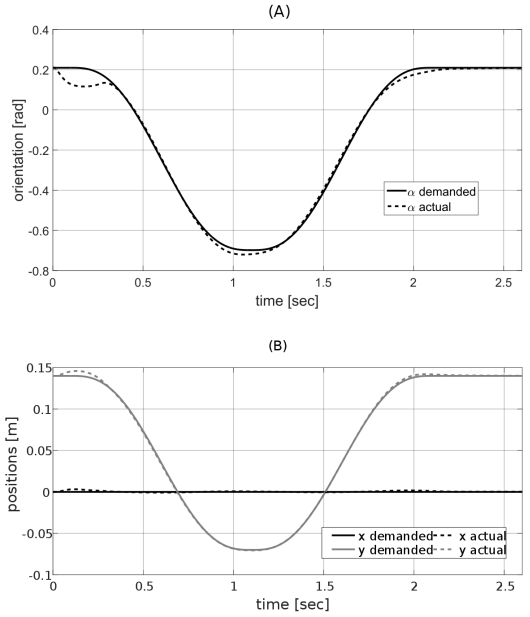

Fig. 9: Numerical comparison between the reference and actual pose of the redundant manipulator's end-effector under torque disturbance (-1.30 N.m): (A) the end-effector's orientation and (B) the end-effector's translational positions

Experimental tests for evaluating the redundant 3PRRR manipulator have also been performed using the same pick-and-place task under no load disturbance. Figure 10 shows the experimental comparison between the reference and actual pose of the redundant manipulator's end-effector. It can be concluded that the redundant manipulator, exploiting the proposed redundancy resolution scheme, has been capable of tracking this reference due to its capability of avoiding singularities.

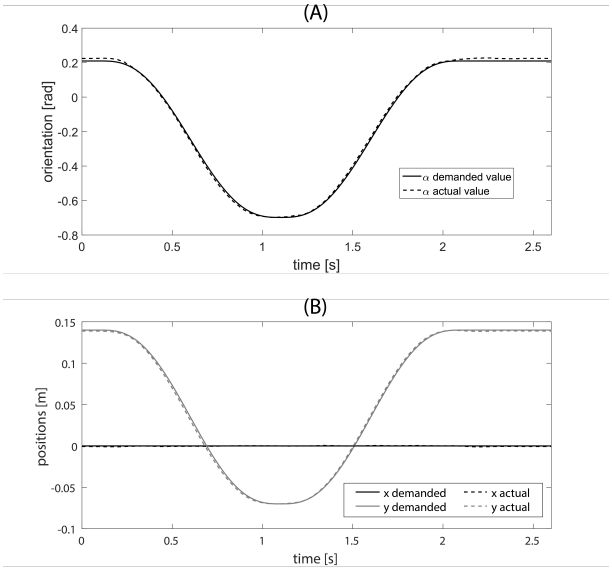

Fig. 10: Experimental comparison between the reference and actual pose of the redundant manipulator's end-effector under no torque disturbance: (A) the end-effector's orientation and (B) the end-effector's translational positions

4.3 Consequences of a proper redundancy resolution scheme

An important consequence of the proposed strategy is the reduction of required maximum torques to perform the required pick-and-place task. Due to its higher rigidity, the actuators of the redundant manipulator are capable of keeping lower current values. A comparison between the required currents of the active revolute joints of the 3RRR and the 3PRRR to perform the pick-and-place task is shown in Fig. 11. The values are considerably reduced for the required pick-and-place task. This result indicates that redundant PKMs can be more energy efficient if proper redundancy resolution schemes are exploited.

The proposed redundancy resolution scheme applied for the motion planning of the 3PRRR to perform the given pick-and-place task was solved using MATLAB installed in a desktop computer with a Intel Processor i5 2.90 GHz. The scheme took about 1.5s indicating that further considerations should be made for improving the computational effort.

5 Conclusions

In this manuscript, a redundancy resolution strategy for kinematically redundant PKMs is proposed. This strategy exploits a Gradient Projection Method for deriving an optimal motion of the redundant actuators. Since this motion may require unrealistic acceleration values, a Differential Dynamic Programming strategy is employed to address the trade-off between acceleration values and tracking performance.

The proposed strategy has been exploited for the redundancy resolution of the redundant 3PRRR planar manipulator. Due to its kinematic architecture, appropriate cost functions have been selected for employing the Gradient projec-

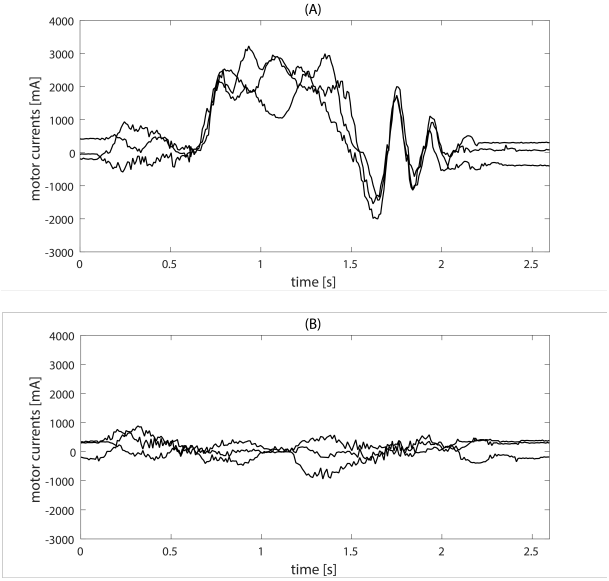

Fig. 11: Active revolute joints' currents: (A) 3RRR and (B) 3PRRR

tion Methods. These cost functions guarantee the avoidance of the singularity regions and the imposition of the geometrical constraints.

Numerical and experimental results have been obtained using the proposed strategy validating the proposal. Using the redundancy resolution scheme, singularity regions have been avoided and the required torques have been reduced.

The methodology seems to be versatile since different cost functions and weighting factors can be selected by the designer.

Alternative approaches for the proposal can be investigated in future research. For instance, the direct use of DDP and the proposal of constraints limiting jerk and acceleration values or the use of iterative Linear Quadratic Gaussian (iLQG) could yield improved results. Moreover, the impact of redundancies in the dynamic performance and/or energy consumption of PKMs should also be further addressed.

6 Acknowledgments

This research is supported by FAPESP 2014/01809-0. Moreover, João C. Santos is thankful for his grant, FAPESP 2014/21946-2.

References

[1] Luces, M., Boyraz, P., Mahmoodi, M., Keramati, F., Mills, J. K., and Benhabib, B., 2016. "An emulator-based prediction of dynamic stiffness for redundant parallel kinematic mechanisms". *ASME Journal of Mechanisms and Robotics,* **8**(2), pp. 021021–15.

[2] Wu, J., Wang, J., and You, Z., 2011. "A comparison study on the dynamics of planar 3-DOF 4-RRR, 3-RRR and 2-RRR parallel manipulators". *Robotics and Computer-Integrated Manufacturing,* **27**(1), Feb., pp. 150–156.

[3] Fontes, J. V., and da Silva, M. M., 2016. "On the dynamic performance of parallel kinematic manipulators with actuation and kinematic redundancies". *Mechanism and Machine Theory,* **103**, pp. 148–166.

[4] Wu, J., Zhang, B., and Wang, L., 2016. "A measure for evaluation of maximum acceleration of redundant and nonredundant parallel manipulators". *ASME Journal of Mechanisms and Robotics,* **8**(2), pp. 021001–8.

[5] Müller, A., 2016. "Local kinematic analysis of closed-loop linkages mobility, singularities, and shakiness". *ASME Journal of Mechanisms and Robotics,* **8**(4), p. 041013.

[6] Kotlarski, J., Abdellatif, H., Ortmaier, T., and Heimann, B., 2009. "Enlarging the useable workspace of planar parallel robots using mechanisms of variable geometry". In Reconfigurable Mechanisms and Robots, 2009. ReMAR 2009. ASME/IFToMM International Conference on, pp. 63–72.

[7] Paccot, F., Andref, N., and Martinet, P., 2009. "Review on the dynamic control of parallel kinematic machines: Theory and experiments". *The International Journal of Robotics Research,* **28**(3), pp. 395–416.

[8] Bourbonnais, F., Bigras, P., and Bonev, I. A., 2015. "Minimum-time trajectory planning and control of a pick-and-place five-bar parallel robot". *IEEE/ASME Transactions on Mechatronics,* **20**(2), April, pp. 740–749.

[9] Lakhal, O., Melingui, A., and Merzouki, R., 2016. "Hybrid approach for modeling and solving of kinematics of a compact bionic handling assistant manipulator". *IEEE/ASME Transactions on Mechatronics,* **21**(3), pp. 1326–1335.

[10] da Silva, M. M., de Oliveira, L. P., Bruls, O., Michelin, M., Baradat, C., Tempier, O., Caigny, J. D., Swevers, J., Desmet, W., and Brussel, H. V., 2010. "Integrating structural and input design of a 2-dof high-speed parallel manipulator: A flexible model-based approach". *Mechanism and Machine Theory,* **45**(11), pp. 1509 – 1519.

[11] Ahuactzin, J. M., and Gupta, K. K., 1999. "The kinematic roadmap: a motion planning based global approach for inverse kinematics of redundant robots". *IEEE Transactions on Robotics and Automation,* **15**(4), Aug, pp. 653–669.

[12] Cha, S.-H., Lasky, T. A., and Velinsky, S. A., 2007. "Singularity Avoidance for the 3-RRR Mechanism Using Kinematic Redundancy". In Proceedings 2007 IEEE International Conference on Robotics and Automation, IEEE, pp. 1195–1200.

[13] Muller, A., 2008. "On the Terminology for Redundant Parallel Manipulators". In Volume 2: 32nd Mechanisms and Robotics Conference, Vol. 2, ASME, pp. 1121–1130.

[14] Ebrahimi, I., Carretero, J. A., and Boudreau, R., 2006. "Workspace comparison of kinematically redundant planar parallel manipulators". In *Romansy 16*. Springer, pp. 89–96.

[15] Kotlarski, J., Heimann, B., and Ortmaier, T., 2011.

"Experimental validation of the influence of kinematic redundancy on the pose accuracy of parallel kinematic machines". In Robotics and Automation (ICRA), 2011 IEEE International Conference on, pp. 1923–1929.

[16] Xie, F., Liu, X.-J., and Wang, J., 2011. "Performance Evaluation of Redundant Parallel Manipulators Assimilating Motion/Force Transmissibility". *International Journal of Advanced Robotic Systems,* **8**(5), pp. 113–124.

[17] Ruiz, A. G., Fontes, J. V. C., and da Silva, M. M., 2015. "The Impact of Kinematic and Actuation Redundancy on the Energy Efficiency of Planar Parallel Kinematic Machines". In Proceedings of 17th International Symposium on Dynamic Problems of Mechanics.

[18] Ukidve, C. S., McInroy, J. E., and Jafari, F., 2008. "Using redundancy to optimize manipulability of stewart platforms". *IEEE/ASME Transactions on Mechatronics,* **13**(4), pp. 475–479.

[19] Siciliano, B., 1990. "Kinematic control of redundant robot manipulators: A tutorial". *Journal of lntelligent and Robotic Systems,* **3**(3), pp. 201–212.

[20] Shin, K., and maKay, N. D., 1986. "A dynamic programming approach to trajectory planning of robotic manipulators". *IEEE Transactions on Automatic Control,* **31**(6), pp. 491–500.

[21] Nakamura, Y., and Hanafusa, H., 1987. "Optimal redundancy control of redundant manipulators". *The International Journal of Robotics Research,* **6**(1), pp. 32–42.

[22] Martin, D. P., Baillieul, J., and Hollerbach, J. M., 1989. "Resolution of kinematic redundancy using optimization techniques". *IEEE Transactions on Robotics and Automation,* **5**(4), pp. 529–533.

[23] Deb, K., Agrawal, S., Pratap, A., and Meyarivan, T., 2002. "A fast elitist non-dominated sorting genetic algorithm for multi-objective optimization: Nsga-ii". *IEEE Transactions on the Evolutionary Computation,* **6**, pp. 182–197.

[24] Marcos, M. G., Machado, J. A. T., and Azevedo-Perdicoúlis, T.-P., 2012. "A multi-objective approach for the motion planning of redundant manipulators". *Applied Soft Computing,* **12**(2), pp. 589 – 599.

[25] Kim, H., Miller, L. M., Byl, N., Abrams, G., and Rosen, J., 2012. "Redundancy resolution of the human arm and an upper limb exoskeleton". *IEEE Transactions on Biomedical Engineering,* **59**(6), pp. 1770–1779.

[26] Minami, M., X, X. L., Matsuno, T., and Yanou, A., 2016. "Dynamic reconfiguration manipulability for redundant manipulators". *ASME Journal of Mechanisms and Robotics,* **8**(6), pp. 061004–9.

[27] Kotlarski, J., Thanh, T. D., Heimann, B., and Ortmaier, T., 2010. "Optimization strategies for additional actuators of kinematically redundant parallel kinematic machines". In Robotics and Automation (ICRA), 2010 IEEE International Conference on, pp. 656–661.

[28] Thanh, T. D., Kotlarski, J., Heimann, B., and Ortmaier, T., 2012. "Dynamics identification of kinematically redundant parallel robots using the direct search method". *Mechanism and Machine Theory,* **52**, pp. 277 – 295.

[29] Boudreau, R., and Nokleby, S., 2012. "Force optimization of kinematically-redundant planar parallel manipulators following a desired trajectory". *Mechanism and Machine Theory,* **56**, oct, pp. 138–155.

[30] Bellman, R., 2003. *Dynamic Programming*. Dover Publications.

[31] Guigue, A., Ahmadi, M., Hayes, M., Langlois, R., and Tang, F., 2007. "A dynamic programming approach to redundancy resolution with multiple criteria". In Proceedings 2007 IEEE International Conference on Robotics and Automation, IEEE, pp. 1375–1380.

[32] Nakamura, Y., and Hanafusa, H., 1986. "Inverse kinematic solutions with singularity robustness for robot manipulator control". *ASME Journal of Journal of Dynamic Systems, Measurement, and Control,* **108**(3), pp. 163–171.

[33] Cahill, A. J., James, M. R., Kieffer, J. C., and Williamson, D., 1998. "Remarks on the application of dynamic programming to the optimal path timing of robot manipulators". *International Journal of Robust and Nonlinear Control,* **8**(6), pp. 463–482.

[34] Tassa, Y., Mansard, N., and Todorov, E., 2014. "Control-limited differential dynamic programming". In 2014 IEEE International Conference on Robotics and Automation (ICRA), pp. 1168–1175.

[35] Rao, S. S., 2009. *Engineering Optimization: Theory and Practice*, fourth edition ed. Wiley, New Jersey.

[36] Patel, S., and Sobh, T., 2015. "Manipulator performance measures - a comprehensive literature survey". *Journal of Intelligent & Robotic Systems,* **77**(3), pp. 547–570.

List of figure captions

Fig. 1: 3PRRR: the kinematically redundant planar parallel manipulator built at São Carlos School of Engineering at University of São Paulo

Fig. 2: Schematic representation of a 3PRRR

Fig. 3: 3RRR: (A) non-singular configuration and (B) singular configuration, which mitigates mechanism rigidity

Fig. 4: Illustration of persistent interchange between σ_2 and σ_3

Fig. 5: The influence of c_3 over H_3

Fig. 6: Pick-and-place task: reference poses

Fig. 7: Numerical results: comparison between the reference and actual poses of the non-redundant manipulator's end-effector under torque disturbance (-0.05 N.m)

Fig. 8: Experimental results: comparison between (A) the reference final pose and (B) the actual final pose of the non-redundant manipulator under no load disturbance

Fig. 9: Numerical comparison between the reference and actual pose of the redundant manipulator's end-effector under torque disturbance (-1.30 N.m): (A) the end-effector's orientation and (B) the end-effector's translational positions

Fig. 10: Experimental comparison between the reference and actual pose of the redundant manipulator's end-effector under no torque disturbance: (A) the end-effector's orientation and (B) the end-effector's translational positions

Fig. 11: Active revolute joints' currents: (A) 3RRR and (B) 3PRRR

List of table captions

Table 1: Dimensions of the prototype

Table 2: Weighting terms